Extended Reduced-order surrogate models for scalar-tensor gravity in the strong field and applications to binary pulsars and gravitational wave*

Minghao Guo, Junjie Zhao,† and Lijing Shao‡
Peking University, Beijing 100871, China
(MUSO Collaboration)
(Dated: October 30, 2020)

An article usually includes an abstract, a concise summary of the work covered at length in the main body of the article.

Usage: Secondary publications and information retrieval purposes.

Structure: You may use the `description` environment to structure your abstract; use the optional argument of the `\item` command to give the category of each item.

I. INTRODUCTION

This sample document demonstrates proper use of REVTEX 4.2 (and LATEX 2_ε) in mansucripts prepared for submission to APS journals. Further information can be found in the REVTEX 4.2 documentation included in the distribution or available at `http://journals.aps.org/revtex/`.

When commands are referred to in this example file, they are always shown with their required arguments, using normal TEX format. In this format, `#1`, `#2`, etc. stand for required author-supplied arguments to commands. For example, in `\section{#1}` the `#1` stands for the title text of the author's section heading, and in `\title{#1}` the `#1` stands for the title text of the paper.

Line breaks in section headings at all levels can be introduced using `\\`. A blank input line tells TEX that the paragraph has ended. Note that top-level section headings are automatically uppercased. If a specific letter or word should appear in lowercase instead, you must escape it using `\lowercase{#1}` as in the word "via" above.

A. Second-level heading: Formatting

This file may be formatted in either the `preprint` or `reprint` style. `reprint` format mimics final journal output. Either format may be used for submission purposes. `letter` sized paper should be used when submitting to APS journals.

1. *Wide text (A level-3 head)*

The `widetext` environment will make the text the width of the full page, as on page **??**. (Note the use the `\pageref{#1}` command to refer to the page number.)

a. Note (Fourth-level head is run in) The width-changing commands only take effect in two-column formatting. There is no effect if text is in a single column.

B. Citations and References

A citation in text uses the command `\cite{#1}` or `\onlinecite{#1}` and refers to an entry in the bibliography. An entry in the bibliography is a reference to another document.

1. *Citations*

Because REVTEX uses the `natbib` package of Patrick Daly, the entire repertoire of commands in that package are available for your document; see the `natbib` documentation for further details. Please note that REVTEX requires version 8.31a or later of `natbib`.

a. Syntax The argument of `\cite` may be a single *key*, or may consist of a comma-separated list of keys. The citation *key* may contain letters, numbers, the dash (-) character, or the period (.) character. New with natbib 8.3 is an extension to the syntax that allows for a star (*) form and two optional arguments on the citation key itself. The syntax of the `\cite` command is thus (informally stated)

`\cite` { *key* }, or
`\cite` { *optarg+key* }, or
`\cite` { *optarg+key* , *optarg+key*… },

where *optarg+key* signifies

key, or
**key*, or
`[`*pre*`]`*key*, or
`[`*pre*`][`*post*`]`*key*, or even
`*[`*pre*`][`*post*`]`*key*.

where *pre* and *post* is whatever text you wish to place at the beginning and end, respectively, of the bibliographic reference (see Ref. [1] and the two under Ref. [2]). (Keep in mind that no automatic space or punctuation is applied.) It is highly recommended that you put the entire *pre* or *post* portion within its own set of braces, for example: `\cite { [ {`*text*`}]`*key*`}`. The extra set of braces will keep LATEX out of trouble if your *text* contains the comma (,) character.

The star (*) modifier to the *key* signifies that the reference is to be merged with the previous reference into a single bibliographic entry, a common idiom in APS and AIP articles (see

---

* A footnote to the article title
† Second.Author@institution.edu
‡ lshao@pku.edu.cn

below, Ref. [2]). When references are merged in this way, they are separated by a semicolon instead of the period (full stop) that would otherwise appear.

b. Eliding repeated information When a reference is merged, some of its fields may be elided: for example, when the author matches that of the previous reference, it is omitted. If both author and journal match, both are omitted. If the journal matches, but the author does not, the journal is replaced by *ibid.*, as exemplified by Ref. [2]. These rules embody common editorial practice in APS and AIP journals and will only be in effect if the markup features of the APS and AIP BibTEX styles is employed.

c. The options of the cite command itself Please note that optional arguments to the *key* change the reference in the bibliography, not the citation in the body of the document. For the latter, use the optional arguments of the `\cite` command itself: `\cite` `*`[*pre-cite*][*post-cite*]{*key-list*}.

2. Example citations

By default, citations are numerical[3]. Author-year citations are used when the journal is RMP. To give a textual citation, use `\onlinecite{#1}`: Refs. 1 and 4. By default, the `natbib` package automatically sorts your citations into numerical order and "compresses" runs of three or more consecutive numerical citations. REVTEX provides the ability to automatically change the punctuation when switching between journal styles that provide citations in square brackets and those that use a superscript style instead. This is done through the `citeautoscript` option. For instance, the journal style `prb` automatically invokes this option because *Physical Review B* uses superscript-style citations. The effect is to move the punctuation, which normally comes after a citation in square brackets, to its proper position before the superscript. To illustrate, we cite several together [1, 2, 4–6], and once again in different order (Refs. [1, 2, 4–6]). Note that the citations were both compressed and sorted. Futhermore, running this sample file under the `prb` option will move the punctuation to the correct place.

When the `prb` class option is used, the `\cite{#1}` command displays the reference's number as a superscript rather than in square brackets. Note that the location of the `\cite{#1}` command should be adjusted for the reference style: the superscript references in `prb` style must appear after punctuation; otherwise the reference must appear before any punctuation. This sample was written for the regular (non-`prb`) citation style. The command `\onlinecite{#1}` in the `prb` style also displays the reference on the baseline.

3. References

A reference in the bibliography is specified by a `\bibitem{#1}` command with the same argument as the `\cite{#1}` command. `\bibitem{#1}` commands may be crafted by hand or, preferably, generated by BibTEX. REVTEX 4.2 includes BibTEX style files `apsrev4-2.bst`, `apsrmp4-2.bst` appropriate for *Physical Review* and *Reviews of Modern Physics*, respectively.

4. Example references

This sample file employs the `\bibliography` command, which formats the `output.bbl` file and specifies which bibliographic databases are to be used by BibTEX (one of these should be by arXiv convention `output.bib`). Running BibTEX (via `bibtex output`) after the first pass of LATEX produces the file `output.bbl` which contains the automatically formatted `\bibitem` commands (including extra markup information via `\bibinfo` and `\bibfield` commands). If not using BibTEX, you will have to create the `thebibiliography` environment and its `\bibitem` commands by hand.

Numerous examples of the use of the APS bibliographic entry types appear in the bibliography of this sample document. You can refer to the `output.bib` file, and compare its information to the formatted bibliography itself.

C. Footnotes

Footnotes, produced using the `\footnote{#1}` command, usually integrated into the bibliography alongside the other entries. Numerical citation styles do this[1]; author-year citation styles place the footnote at the bottom of the text column. Note: due to the method used to place footnotes in the bibliography, *you must re-run BibTEX every time you change any of your document's footnotes*.

II. SPONTANEOUS SCALARIZATION IN THE DEF THEORY

In this section, we study the DEF theory, which is defined by the following general action in *Einstein frame* [7, 8],

$$\begin{aligned} S =& \frac{c^4}{16\pi G_\star}\int \frac{\mathrm{d}^4 x}{c}\sqrt{-g_\star}\left[R_\star - 2g_\star^{\mu\nu}\partial_\mu\varphi\partial_\nu\varphi - V(\varphi)\right] \\ &+S_m[\psi_m; A^2(\varphi)g^\star_{\mu\nu}]\,. \end{aligned} \tag{1}$$

Here, $G_\star$ denotes the bare gravitational constant, $g_\star \equiv \det g^\star_{\mu\nu}$ is the determinant of Einstein metric $g^\star_{\mu\nu}$, $R_\star$ is the Ricci curvature scalar of $g^\star_{\mu\nu}$, and φ is a dynamical scalar field. In the last term of Eq. (1), ψ_m denotes matter fields collectively, and the conformal coupling factor $A(\varphi)$ describes how φ couples to ψ_m in Einstein frame. Varying the action (1) yields the field equations,

$$R^\star_{\mu\nu} =\partial_\mu\varphi\partial_\nu\varphi + \frac{8\pi G_\star}{c^4}\Big(T^\star_{\mu\nu} - \frac{1}{2}T^\star g^\star_{\mu\nu}\Big)\,, \tag{2}$$

$$\Box_{g^\star}\varphi =-\frac{4\pi G_\star}{c^4}\alpha(\varphi)T_\star\,, \tag{3}$$

[1] Automatically placing footnotes into the bibliography requires using BibTeX to compile the bibliography.

where $T_\star^{\mu\nu} \equiv 2c(-g_\star)^{-1/2}\delta S_m/\delta g^\star_{\mu\nu}$ denotes the matter stress-energy tensor, and $T^\star \equiv g^\star_{\mu\nu}T_\star^{\mu\nu}$ is the trace. In Eq. (3), the quantity $\alpha(\varphi)$ is defined as the logarithmic derivative of $A(\varphi)$,

$$\alpha(\varphi) \equiv \frac{\partial \ln A(\varphi)}{\partial\varphi}\,, \tag{4}$$

which indicates the coupling strength between the scalar field and matters.

In the DEF theory [8], $\ln A(\varphi)$ is designated as

$$\ln A(\varphi) = \frac{1}{2}\beta_0\varphi^2\,. \tag{5}$$

Then $\alpha(\varphi) = \partial \ln A(\varphi)/\partial\varphi = \beta_0\varphi$. We designate $\alpha_0 \equiv \beta_0\varphi_0$, where φ_0 is the asymptotic scalar field value of φ at spatial infinity. Note that we have $\alpha_0 = \beta_0 = 0$ in GR.

For NSs, nonperturbative scalarization phenomena develop when [7, 9]

$$\beta_0 \equiv \left.\frac{\partial^2 \ln A(\varphi)}{\partial\varphi^2}\right|_{\varphi=\varphi_0} \lesssim -4\,. \tag{6}$$

Generally, a more negative β_0 means more manifest spontaneous scalarization in the strong-field regime. In such case, the *effective scalar coupling* for a NS "A" with Arnowitt–Deser–Misner (ADM) mass m_A is

$$\alpha_A \equiv \left.\frac{\partial \ln m_A(\varphi)}{\partial\varphi}\right|_{\varphi=\varphi_0}\,, \tag{7}$$

which measures the coupling strength between the scalar field and the NS.

Now we consider a scalarized NS in a binary pulsar system. For a NS binary system with the pulsar labeled "A" and its companion labeled "B", the quantities α_A and α_B contribute to the secular change of the orbital period decay $\dot{P}_b$ [8].Should I wirte the exact formula here? Correspondingly, we define

$$\beta_A \equiv \left.\frac{\partial\alpha_A}{\partial\varphi}\right|_{\varphi=\varphi_0}\,, \tag{8}$$

which is the strong-field analogue of the quantity β_0. Then the theoretical prediction for the periastron advance rate is [8]

$$\dot{\omega}^{\rm th}(m_A, m_B) \equiv \frac{3n_b}{1-e^2}\left(\frac{G_{AB}(m_A+m_B)n_b}{c^3}\right)^{2/3} \times\left[\frac{1-\frac{1}{3}\alpha_A\alpha_B}{1+\alpha_A\alpha_B} - \frac{X_A\beta_B\alpha_A^2 + X_B\beta_A\alpha_B^2}{6(1+\alpha_A\alpha_B)^2}\right], \tag{9}$$

where $n_b \equiv 2\pi/P_b$, $G_{AB} \equiv G_\star(1+\alpha_A\alpha_B)$, and $X_A \equiv m_A/(m_A+m_B) \equiv 1 - X_B$. Finally, consider a NS with inertia moment (in Einstein units) I_A. We denote

$$k_A \equiv \left.\frac{\partial \ln I_A}{\partial\varphi}\right|_{\varphi=\varphi_0} \tag{10}$$

as the "coupling factor" of inertia moment. The theoretical prediction of the Einstein delay parameter is [8],

$$\gamma \equiv \gamma^{\rm th}(m_A, m_B) = \frac{e}{n_b}\frac{X_B}{1+\alpha_A\alpha_B}\left(\frac{G_{AB}(m_A+m_B)n_b}{c^3}\right)^{2/3} \times[X_B(1+\alpha_A\alpha_B) + 1 + K_A^B]\,, \tag{11}$$

where $K_A^B \equiv -\alpha_B(m_B)k_A(m_A)$ describes the contribution from the variation of I_A under the influence of the companion B.

Maybe add a discussion about what kind of system (like binary NS) should be applied?

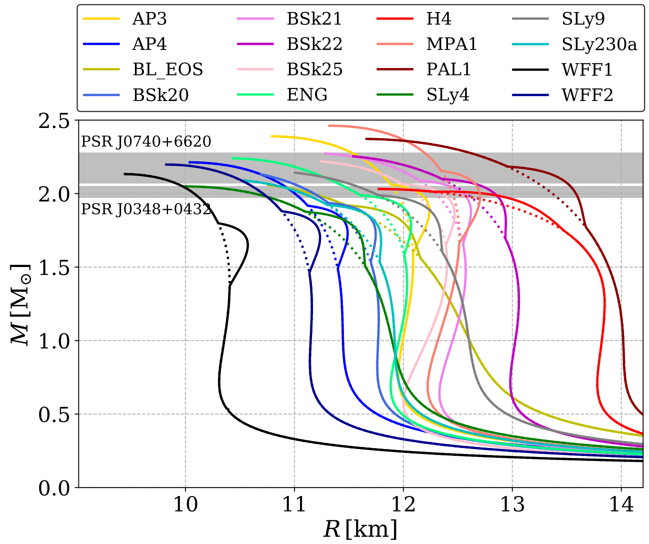

FIG. 1. Mass-radius relations of NSs for the EOSs that we adopt in this study. The mass-radius relations are derived from GR (dashed lines) and from a DEF theory with $\log_{10}|\alpha_0| = -5.0$ and $\beta_0 = -4.5$ (solid lines). The masses from PSRs J0740+6620 and J0348+0432 are overlaid in grey. The "bumps" show the deviation of the DEF theory from GR.

III. METHODOLOGY

We here turn our attention to the calculation of the quantities in strong field. For a specific nuclear EOS of NSs, given the center mass density ρ_c and the parameters of the theory (namely, α_0, β_0), we can obtain macroscopic quantities of a NS (e.g, R, m_A, α_A and I_A), by solving the modified TOV equations with the shooting method (see Ref. [10] for details). In Fig. 1 we show mass-radius relation of NSs in the DEF theory with $\log_{10}|\alpha_0| = -5.0$ and $\beta_0 = -4.5$ for the EOSs we adopt in this study. It shows clearly that the spontaneous scalarization phenomena develop for NSs with certain masses, and lager radii are predicted in this range. However, to determine quantities β_A and k_A, we have to calculate the derivatives from Eqs. (8) and (10) for a fixed form of the conformal coupling factor $A(\varphi)$ (i.e, with a fixed β_0) and a fixed baryonic mass $\bar{m}_A$. This requires the data with different φ_0's (or equivalently, α_0's). In order to do so, we calculate the derivatives on

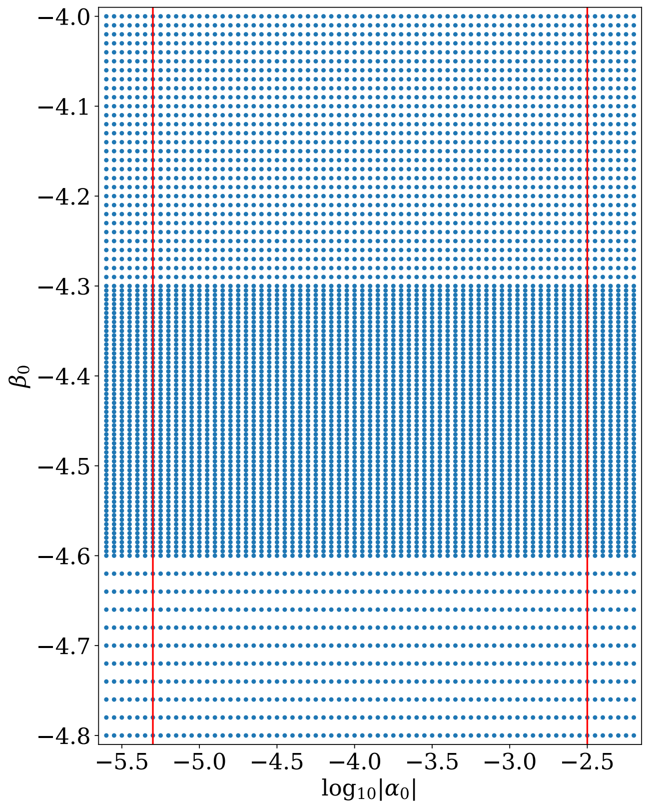

FIG. 2. An uneven grid in the parameter space ($\log_{10}|\alpha_0|, -\beta_0$) for calculating β_A and k_A and building ROMs. We generate a set of $69 \times 101 = 6969$ parameter pairs as the training data. The region between red lines corresponds to the data we use in later calculation.

a grid. Should I show the PSR data in Fig.1? Also probably some data about the radius of NS.

In practice, for each EOS, we choose the range of ρ_c so that $m_A \in (1\,\mathrm{M}_\odot, m_A^{\max})$ with the maximum NS mass $m_A^{\max}$ being EOS-dependent. Then we generate an uneven gird of $[\log_{10}|\alpha_0|, \beta_0] \in [-5.6, -2.2] \times [-4.8, -4.0]$, as shown in Fig. 2. The number of nodes in grid is set to $N_{\alpha_0} \times N_{\beta_0} = 69 \times 101 = 6969$. We calculate β_A and k_A on each node with a reasonable differential step. Finally, we use the data of $\log_{10}|\alpha_0| \in [-5.3, -2.5]$ for further calculation to avoid the inaccuracy of derivatives at boundaries. The boundary value $\alpha_0 \approx 10^{-2.5}$ is the upper limit given by the Cassini spacecraft [11], and $\beta_0 \lesssim -4.0$ corresponds to values where spontaneous scalarization happens in the DEF theory.

We have to point it out that in practice it is difficult to calculate k_A when the scalar field is weak. In this case, a change in I_A due to the weak field is comparable to the random noises during the integration in solving the modified TOV equations. The calculation of k_A is therefore not accurate. Here we propose a reasonable approximation that $k_A \sim \varphi_0^2$ when the spontaneous scalarization is not excited. Based on this assumption, we choose a large differential step and calculate $k_A = 2\varphi\partial \ln I_A/\partial\varphi^2$ to reduce the influence of numerical noises.

Due to the time-consuming computation of the TOV integration and the shooting method for large-scale calculations, such as the parameter estimation with the MCMC approach, we build ROMs for the quantities to improve the efficiency. In brief, to generate a ROM for a curve $h(t;\lambda)$ with parameters λ, one provides a training space of data $\mathbf{V} \equiv \{h(t;\lambda_i)\}$ on a given grid of parameters and select a certain number (denoted as m) of bases as a chosen space $\mathbf{RV} = \{e_i\}_{i=1}^m$ with the reduced basis (RB) method. In practice, given the starting RB ($i = 0$), one iteratively seeks for m orthonormal RBs by iterating the Gram-Schmidt orthogonalization algorithm with greedy selection to minimize the maximum projection error, [LS: references needed]

$$\sigma_i \equiv \max_{h\in\mathbf{V}} \left\| h(\cdot;\lambda) - \mathcal{P}_i h(\cdot;\lambda) \right\|^2, \tag{12}$$

where $\mathcal{P}$ describes the projection of $h(t;\lambda)$ onto the span of the first i RBs. The process terminates when $\sigma_{m-1} \lesssim \Sigma$, a user-specified error bound. Then every curve in the training space is well approximated by

$$h(t;\lambda) \approx \sum_{i=1}^{m} c_i(\lambda) e_i(t) \approx \sum_{i=1}^{m} \langle h(\cdot;\lambda), e_i(\cdot)\rangle e_i(t), \tag{13}$$

where $c_i(\lambda)$ is the coefficient to be used for the ROM. Finally, one performs a fit to the parameter space, $\{\lambda_i\}$, and complete the construction of ROM. More details can be found in Ref. [10] where ROMs of α_A were built.

Extending the work by Zhao *et al.* [10], we build ROMs for six quantities, R, m_A, I_A, α_A, β_A and k_A, as functions of the central mass density ρ_c, with specialized parameters $\lambda = (\alpha_0, \beta_0)$.[2] We choose the implicit parameter ρ_c as an independent variable to avoid the the multivalued relations between m_A and R, as well as α_A and I_A [10]. We show this phenomena in Fig. 3. Due to the multivalued relations, β_A and k_A are negative when the α_A-m_A and I_A-m_A curve are bent backwards.

In balancing the computation cost and the accuracy of ROMs, we set the error bound $\Sigma = 10^{-7}$ for m_A, R and I_A, $\Sigma = 10^{-5}$ for α_A, and $\Sigma = 10^{-4}$ for β_A and k_A. The relative projection error $\tilde{\sigma}_i \equiv \sigma_i/\sigma_0$ as a function of the basis size is shown in Fig. 4. To achieve the desired projection error, the basis size is $\sim$ 20-40 for m_A, R and I_A, but $\sim$ 150-200 for α_A, β_A and k_A. This is due to the fact that there are more features in the latter set of parameters. Considering the error involved in the shooting method and the calculation of derivatives, which is $\sim 1\%$, the precision loss in ROM building is negligible. But, $\varepsilon(k_A)$ is much larger than 0.01, maybe we should point it out. About $\varepsilon(k_A)$, since we build ROM for $\ln|k_A + k_0|$, is it reasonable to build assess the accuracy using Eq. 14?

To assess the accuracy of the ROMs, we define

$$\varepsilon(X) = \left| \frac{X_{\mathrm{ROM}} - X_{\mathrm{mTOV}}}{X_{\mathrm{ROM}} + X_{\mathrm{mTOV}}} \right|, \tag{14}$$

[2] In practice, we use $\ln|I_A|$, $\ln|\alpha_A|$, $\ln|\beta_A|$, and $\ln|k_0 + k_A|$—instead of β_A and k_A—for a better numerical performance, where k_0 is an EOS-dependent constant to avoid negative values of k_A in the weak field. Generally we have $k_0 \lesssim 0.1$.

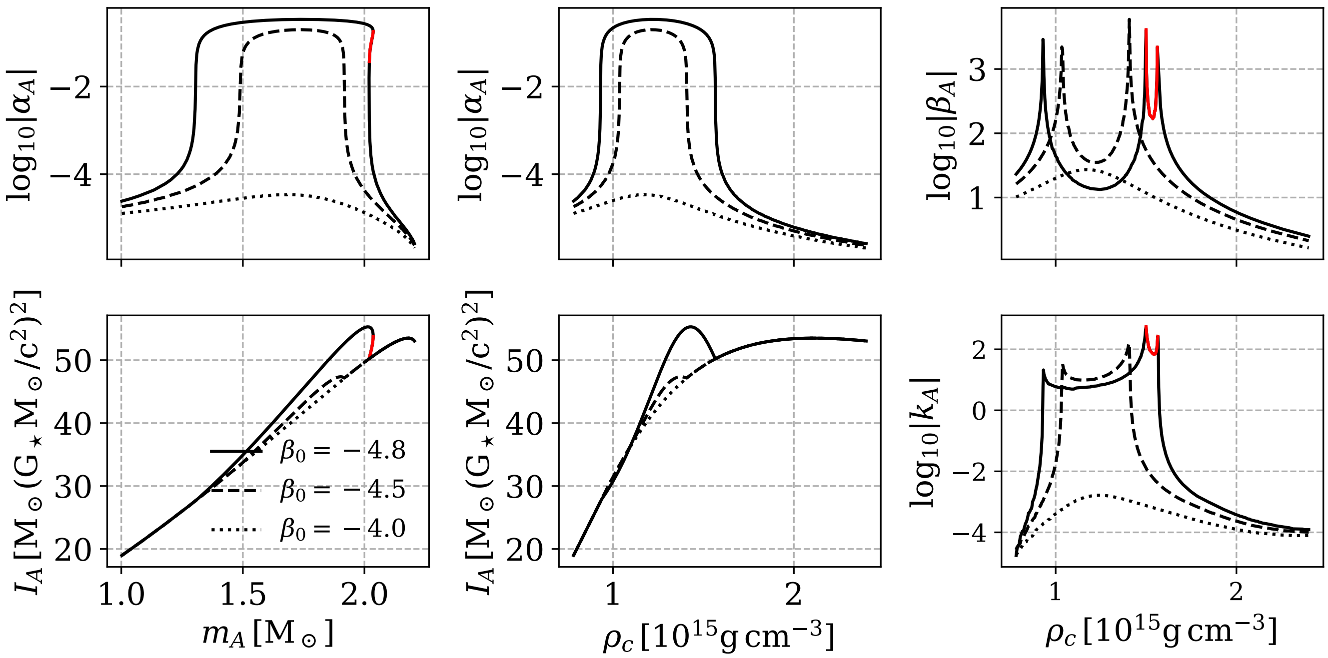

FIG. 3. Pathological phenomena occur when integrating the modified TOV equations for the EOS AP4. The calculation assumes the DEF parameters $\log_{10}|\alpha_0| = -5.3$ and $\beta_0 = -4.8$ (solid lines), -4.5 (dashed lines) and -4.0 (dotted lines). For $\log_{10}|\alpha_0| = -5.3$, the scalar field is weak for $\beta_0 = -4.0$, strong for $\beta_0 = -4.5$, and this causes the pathological phenomena for $\beta_0 = -4.8$. The red lines mark the pathological region. In this region, β_A and k_A are negative.

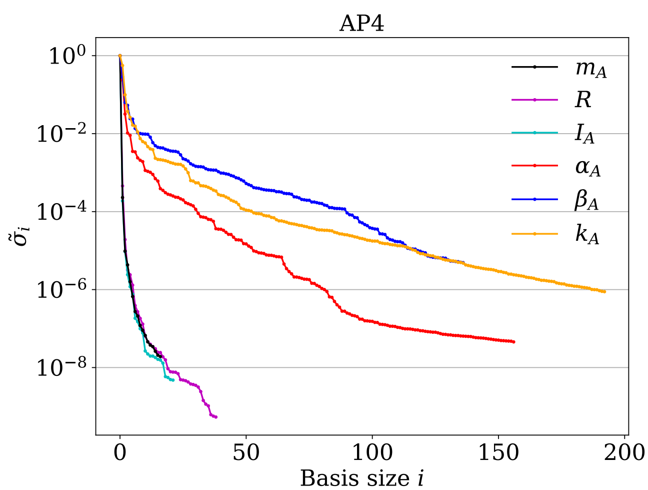

FIG. 4. Relative maximum projection error, $\tilde{\sigma}_i$, in building the ROMs for the EOS AP4. We set $\Sigma = 10^{-7}$ for m_A, R and I_A, $\Sigma = 10^{-5}$ for α_A, and $\Sigma = 10^{-4}$ for β_A and k_A.

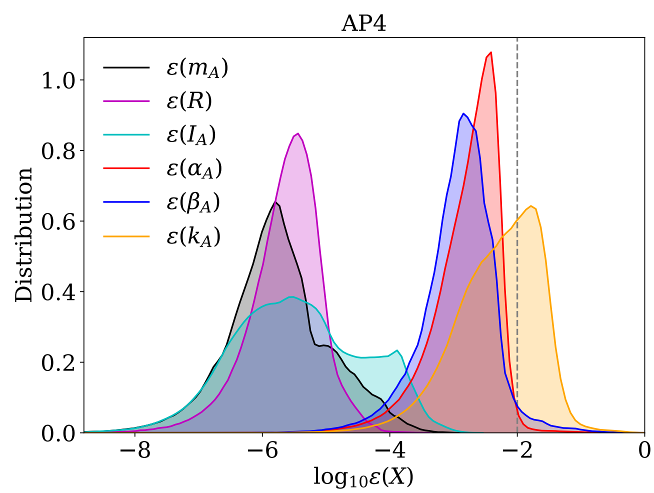

FIG. 5. Kernel density estimation (KDE) distribution of the relative error $\varepsilon(X)$, where $X \in \{m_A, R, I_A, \alpha_A, \beta_A, k_A\}$. The dashed line shows the relative tolerable error in the TOV integration ($\lesssim 1\%$).

where $X \in \{m_A, R, I_A, \alpha_A, \beta_A, k_A\}$, to indicate the fractional accuracy of the ROMs. In Eq. (14), we denote X_{ROM} as the prediction of ROM, and X_{mTOV} as the value from the shooting algorithm and derivatives on the grid. Explain why choosing grid here. To calculate the derivatives, instead of randomly generating parameters, we choose another grid as the test space which is shifted from the training space for α_0, β_0 and ρ_c, and calculate the quantities in the same way. We should explain why we test the parameters shifted in training space instead of random space The test space has sparser distribution of β_0. The distributions of $\varepsilon(X)$ are shown in Fig. 5. The relative errors of m_A, R and I_A are $\lesssim 10^{-5}$. On the contrary, relative errors of α_A, β_A and k_A is mostly smaller than 1%. Although this error is larger than those of R and m_A, in most cases, the error is still small enough to be neglected compared with the error from the shooting method and the calculation of derivatives. About the error: For k_A, due to the additional error from the method in calculating the derivatives, a small fraction of prediction have the error in the range $\sim 1-10\%$.

IV. CONSTRAINTS FROM BINARY PULSARS

To be finished...

In Table I, we show

$$P(\alpha_0,\beta_0|\mathcal{D},\mathcal{H},\mathcal{I}) = \int \frac{P(\mathcal{D}|\alpha_0,\beta_0\Xi,\mathcal{H},\mathcal{I})P(\alpha_0,\beta_0|,\Xi|\mathcal{H},\mathcal{I})}{P(\mathcal{D}|\mathcal{H},\mathcal{I})}\mathrm{d}\Xi\,, \tag{15}$$

[1] E. Witten, (2001), hep-th/0106109, and references therein

[2] See the explanation of time travel in R. P. Feynman, Phys. Rev. **94**, 262 (1954); The classical relativistic treatment of A. Einstein, Yu. Podolsky, and N. Rosen (EPR), *ibid*. **47**, 777 (1935) is a relative classic

[3] E. Beutler, in *Williams Hematology*, Vol. 2, edited by E. Beutler, M. A. Lichtman, B. W. Coller, and T. S. Kipps (McGraw-Hill, New York, 1994) Chap. 7, pp. 654–662, 5th ed.

[4] N. D. Birell and P. C. W. Davies, *Quantum Fields in Curved Space* (Cambridge University Press, 1982).

[5] J. G. P. Berman and J. F. M. Izrailev, Physica D **88**, 445 (1983).

[6] E. B. Davies and L. Parns, Q. J. Mech. Appl. Math. **51**, 477 (1988).

[7] T. Damour and G. Esposito-Farèse, Phys. Rev. Lett. **70**, 2220 (1993).

[8] T. Damour and G. Esposito-Farèse, Phys. Rev. D **54**, 1474 (1996).

[9] E. Barausse, C. Palenzuela, M. Ponce, and L. Lehner, Phys. Rev. D **87**, 081506 (2013).

[10] J. Zhao, L. Shao, Z. Cao, and B.-Q. Ma, Phys. Rev. D **100**, 064034 (2019).

[11] B. Bertotti, L. Iess, and P. Tortora, Nature **425**, 374 (2003).

TABLE I. parameters of binary pulsars.

Name	J0348+0432	J1012+5307	J1738+0333	J1909-3744	J2222-0137
Orbital period, P_b (d)	0.102424062722(7)	0.60467271355(3)	0.3547907398724(13)	1.533449474305(5)	2.44576454(18)
Eccentricity, e	0.0000026(9)	0.0000012(3)	0.00000034(11)	0.000000115(7)	0.00038096(4)
Observed $\dot{P}_b$, $\dot{P}_b^{\rm obs}$ (fs s^{-1})	-273(45)	50(14)	-17.0(31)	-510.87(13)	200(90)
Intrinsic $\dot{P}_b$, $\dot{P}_b^{\rm int}$ (fs s^{-1})	-274(45)	-5(9)	-27.72(64)	-4.4(79)	-60(90)
Periastron advance, $\dot{\omega}$ (deg yr^{-1})	—	—	—	—	0.1001(35)
Einstein delay γ (ms)	—	—	—	—	—
Pulsar mass, m_p (M$_\odot$)	2.01(4)	—	—	1.492(14)	1.76(6)
Companion mass, m_c (M$_\odot$)	$0.1715^{+0.0045}_{-0.0030}$	0.174(7)	$0.1817^{+0.0073}_{-0.0054}$	0.209(1)	1.293(25)
Mass ratio, $q \equiv m_p/m_c$	11.70(13)	10.5(5)	8.1(2)	—	—

TABLE II. parameters of binary pulsars.

Name	B1913+16	J0737-3039A	J1757-1854	B1534+12
Orbital period, P_b (d)	0.322997448918(3)	0.10225156248(5)	0.18353783587(5)	0.420737298879(2)
Eccentricity, e	0.6171340(4)	0.0877775(9)	0.6058142(10)	0.27367752(7)
Observed $\dot{P}_b$, $\dot{P}_b^{\rm obs}$ (fs s^{-1})	-2423(1)	-1252(17)	-5300(200)	-136.6(3)
Intrinsic $\dot{P}_b$, $\dot{P}_b^{\rm int}$ (fs s^{-1})	-2398(4)	-1252(17)	-5300(240)	—
Periastron advance, $\dot{\omega}$ (deg yr^{-1})	4.226585(4)	16.89947(68)	10.3651(2)	1.7557950(19)
Einstein delay γ (ms)	4.307(4)	0.3856(26)	3.587(12)	2.0708(5)
Pulsar mass, m_p (M$_\odot$)	1.438(1)	1.3381(7)	1.3384(9)	1.3330(2)
Companion mass, m_c (M$_\odot$)	1.390(1)	1.2489(7)	1.3946(9)	1.3455(2)
Mass ratio, $q \equiv m_p/m_c$	—	—	—	—